

SENSOR FUSION ON A MINI UNMANNED VEHICLE
INTEGRATING VISION-BASED ALGORITHMS ON AN PARROT AR.DRONE TO AUTONOMOUSLY
FOLLOW LINEAR SHAPED STRUCTURES IN A LANDSCAPE.



Photo by: Parrot SA

A Bachelor Thesis by Camiel R. Verschoor

SENSOR FUSION ON A MINI UNMANNED VEHICLE

INTEGRATING VISION-BASED ALGORITHMS ON AN PARROT AR.DRONE TO AUTONOMOUSLY
FOLLOW LINEAR SHAPED STRUCTURES IN A LANDSCAPE.

Camiel R. Verschoor
10017321

Bachelor thesis
Credits: 18 EC

Bachelor Opleiding Kunstmatige Intelligentie

University of Amsterdam
Faculty of Science
Science Park 904
1098 XH Amsterdam

Supervisors
Dr. A. Visser

Informatics Institute
Faculty of Science
University of Amsterdam
Science Park 904
1098 XH Amsterdam

Drs. G. Poppinga
Defense Systems
Aerospace Systems
National Aerospace Lab
Anthony Fokkerweg 2
1059 CM Amsterdam

July 24th, 2012

Abstract

To be written.

Acknowledgements

I would like to thank my supervisors Arnoud Visser and Gerald Poppinga for their support and guidance. Furthermore, I am grateful to Nick Dijkshoorn for the distribution of his development framework, AR.Drone SLAM, and his support installing it. I also like to thank Robrecht Jurrriaans for borrowing his AR.Drone. Likewise, I would like to thank Rob van Holstein for the construction of a 3D model of the frame that is holding the mirror. Moreover, I like to thank Christian Muller for helping collecting the dataset and learning me to fly a quadcopter manually. Furthermore, I am grateful to the National Aerospace Lab for the internship and the visit to the International Micro Aerial Vehicle Conference and Competitions. Lastly, I am thankful to my girlfriend and my family for their support and encouragement.

Contents

1	Introduction	1
1.1	International Micro Aerial Vehicle Conference and Competitions	2
1.2	Platform and Framework	2
1.3	Research questions and objectives	3
1.4	Outline	3
2	Theory: Vision and Navigation	4
2.1	Edge Detector Algorithm	4
2.1.1	Colour Filter	4
2.1.2	Canny Edge Detector	5
2.2	Motion Detection Algorithm	7
2.2.1	Shi-Thomasi	7
2.2.2	Optical Flow	7
2.2.3	Fundamental Matrix with RANSAC	8
2.2.4	Hartley's algorithm	9
2.2.5	Stereo Matching	9
2.3	Probabilistic Hough Transform	9
2.4	Tracking	10
2.5	Navigation	10
3	Related Work	11
4	Platform: Parrot AR.Drone	13
4.1	Quadcopter	13
4.2	Hardware	14
4.2.1	AR.Drone 1.0	14
4.2.2	AR.Drone 2.0	15
4.3	Software Development Kit	15
5	Framework: AR.Drone SLAM	16
5.1	Functionalities	16
5.2	Architecture	16
6	Methods and Experiments	18
6.1	Platform	18
6.2	Optimal Camera Configuration	18
6.3	Determining line to follow	18
6.4	Experiments	18
6.5	Evaluation Criteria	19
6.6	Hypothesis	19
7	Results and Discussion	20
8	Conclusion	21
8.1	Future works	21
A	Appendices	22
A	Source code	22

B Gaussian Smoothing	23
C Ascending Technologies Pelican	24
9 Bibliography	25

1 Introduction

In robotics one of the main goals is to develop mobile robots that can operate autonomously in the real world environment. These autonomous robots have various purposes and are used for a wide range of applications such as inspection, exploration and rescue. In rescue, robots are expected to operate in dangerous environments without putting human lives at risk for example, during disasters or life rescue operations. Even though reasonable developments have been made in the robotics field, robots cannot operate autonomously in the real world yet.

One of the main requirements of an autonomous robot is the ability to navigate in the operational environment. The traditional approach to navigate through the outdoor environment is via pre-planned paths based on a Global Positioning System (GPS). The main shortcoming of GPS is that it cannot be used in every environment as it needs to receive data signals from at least four different satellites [Bajaj et al., 2002]. Inside buildings and in several outdoor areas GPS is not convenient for navigation. In urban areas GPS is found to be especially unreliable. In order to navigate through these environments other sensors and navigation techniques need to be applied. Since there are several linear structures in the environment such as rivers, roads and power lines, line-following is one possible approach to navigate through an environment. Line-following is a classic technique in robotics as it has been successfully used for ground robots numerous times [Sampei et al., 1995, Dupuis and Parizeau, 2006]. For other robots and sensor configurations, open problems still remain. One of these is navigation for micro aerial vehicles (MAVs), which have a limited sensor composition due to their limited payload. For MAVs line-following is a greater challenge due to the extra dimension it can move in comparing to the average ground robot. Where the sensors of a ground robot can rely on the stability of the ground, while the sensors of a MAV have to count on the stability of the platform during a flight. Therefore, MAV are more likely to measure noisy data, which interpreting algorithms should resist.



Figure 1: The Black Widow [Grasmeyer et al., 2001] was the first operating micro aerial vehicle system, a development which was finalized in 1999 by AeroVironment for Defense Advanced Research Projects Agency (DARPA). The Black Widow can fly for up to 20 minutes and carries a very small color video camera.

A micro aerial vehicle (MAV) is a subclass of the Unmanned Aerial Vehicles. Due to their small size, the MAV can operate in numerous robotic applications, for instance, search & rescue, inspection and exploration. AeroVironment Black Widow[Grasmeyer et al., 2001] (figure 1) is the first MAV operating in the field. Another type of MAV is the quadcopter, which is controlled by four rotors. Quadcopters provide manoeuvrability and stability, which is suitable for indoor and urban flights. As a result of recent developments, small quadcopters with on-board stabilization can be purchased conveniently. Due to this, the research regarding this platform is moving

towards intelligent applications, which demand information of the surrounding environment. Nevertheless, the fast movements and the limited amount of sensor combination mean that it is still a challenge to develop navigation methods for these platforms.

1.1 International Micro Aerial Vehicle Conference and Competitions

The International Micro Aerial Vehicle (IMAV)¹ conference and competitions is an initiative that attempts to share and demonstrate new MAV technology. The competitions emphasizes on flight dynamics and autonomous flight. The IMAV consists of an indoor and outdoor competition, where these aspects are extensively tested in the various challenges. The high level of autonomy is stimulated in this competition as the rules give significantly more points to teams that operate autonomous flights. One of the problems participants have to solve is autonomous navigation through the environment. Although teams are allowed to used visual aids (ie. markers) problems in this area remain. The possible contribution of this thesis to the IMAV competition is a vision-based navigation technique for following linear-shaped objects. This navigation technique can aid autonomous flights during the challenges of the IMAV.

1.2 Platform and Framework

The Parrot AR.Drone (figure 2) is a wireless controlled flying quadcopter built by the French company Parrot SA². The quadcopter is made of plastic and foam and is about 30 centimetres long. It carries a horizontal and a vertical camera opening the door for the development of various visual applications. The inertial measurement unit in combination with optical flow and a ultrasound sensor provide on-board stabilization during flights allowing the quadcopter to hover in the same place.



Figure 2: The Parrot AR.Drone is equipped with two cameras and several inertial sensors. The development is driven by commercial, government, research and military purposes. The small quadrotor allows remote observation of hazardous environments inaccessible for humans and ground robots.

AR.Drone SLAM [Dijkshoorn, 2012] is a development framework for the Parrot AR.Drone, a quadcopter, developed and proposed by N. Dijkshoorn. This framework contains a real-time Simultaneous Localization and Mapping (SLAM) implementation based on a down-pointing camera. Therefore, it allows a MAV to know its position and movement in the environment by generating a feature map of the environment so the MAV can localize itself on this map. Furthermore, the framework contains a 3D mouse controller, a keyboard controller, a visual map

¹<http://www.imav2012.org/>

²<http://www.parrot.com>

and an elevation map. Due to the framework the robot acquires more information of the environment compared to the software of the manufacturer. This information can aid the robot in navigation. In chapter 4 and 5 the platform and framework will be explained.

1.3 Research questions and objectives

In robotics one goal is to develop mobile robots that can advance robustly and truly autonomously in real world situations. One of the main requirements is the ability to navigate autonomously. Since there is no sufficient GPS signal available in urban and indoor environment, robots need to rely on other sensors.

Line-following is proven to be a simple navigation task for ground robots. However, this navigation task is not implemented yet on unmanned aerial vehicles. Since there are various linear structures in the environment, line-following should be a suitable navigation technique.

Therefore, the main research question is to find a robust vision-based approach to autonomously navigate over linear shaped structures. This main research question is divided up in the following sub-questions:

- What is the optimal configuration for the optical sensors of the platform to follow a line?
- What edge and motion detector algorithms are suitable to detect and track a line in a indoor environment?
 - Which algorithms should be tested?
 - Which algorithms should be used?
- What is the performance and robustness of different vision-based methods to navigation over a linear structure in a indoor environment?

In this paper the quality of a edge detection and a motion detection algorithm will be examined to provide an essential component to autonomous behaviour using one camera.

1.4 Outline

Chapter two gives an overview of the the theory this thesis relies on. First, the Computer Vision algorithms this thesis is based on are explained and then the navigation techniques will be discussed. Chapter three gives an overview is given over the related research regarding line-following on unmanned aerial vehicles. The robotic platform, Parrot AR.Drone, is discussed in chapter four. The construction of the platform is explained, the hardware it contains will be listed and the software development kit will be addressed. Chapter five will give an overview of the framework AR.Drone SLAM. The main architecture and functionalities will be briefly discussed. In chapter six the experiments are illustrated and in chapter seven the results will be presented. Chapter eight will discuss the results found in the experiments and elaborate on them. Finally, in chapter nine the conclusion of this thesis will be presented and directions for future research will be proposed.

2 Theory: Vision and Navigation

In this chapter, the basics of the theory this thesis relies on is explained. The work presented in this thesis is based on previous research regarding vision-based algorithms on the AR.Drone [Jurriaans, 2011] and the Open Source Computer Library (OpenCV) [Bradski and Kaehler, 2008], which provides real-time computer vision implementations. Lastly, the navigation techniques will be discussed that interpret the results of the vision techniques.

Over the years various Computer Vision techniques have been developed to detect objects in images. One of the fundamental problems is finding the most applicable algorithm for the defined problem as every algorithm has its advantages and disadvantages. In order to follow a line fast feedback from the camera is required in order for the system to adjust its trajectory. For this reason, a fast and real-time algorithm is favourable. Furthermore, the algorithm should be able to handle movement noise caused by the motions of the flying platform. This thesis will compare a edge-detection approach to a motion-detection approach. Both approaches performance will be tested in combination with a Probabilistic Hough Line Transform [Kiryati et al., 1991], a real-time pattern recognition algorithm to detect lines.

This chapter provides an overview of theory of the Computer Vision algorithms this thesis is based on. A clear explanation will be given over the various algorithms applied in this thesis.

2.1 Edge Detector Algorithm

Edge detection is a tool in Computer Vision that is applied to detect identifying points in a image, where the image brightness discontinuities (see figure 4). A line or linear structure is one of the elements in a image that causes these discontinuities. Due to the wide research over the years to edge detectors there are several implementations [Ziou and Tabbone, 1998]. This thesis will focus on the Canny Edge detector as it is a suitable algorithm for edge detection. The edge detector will be applied to the images in combination with a Colour Filter, which filters out the colours not in range of the filter. This for the reason that only edges containing the same colour as the line need to be detected.

2.1.1 Colour Filter

To filter the colour the colour-space is converted to a different representation, namely, Hue, Saturation and Value (HSV). The HSV colour-space (in figure 3) is a simple transformation of the Red, Green, Blue (RGB) model and a intuitive colour-space, where separate colours can be easily filtered. The Hue stands for the visual sensation according to which an area appears to be similar to one of the perceived colors: red, yellow, green, and blue, or to a combination of two of them. Saturation is the colourfulness of a stimulus relative to its own brightness. Value is the brightness relative to the brightness of a similarly illuminated white. The three parameters have the following ranges: Hue has a range of 0° - 360° , Saturation a range of 0-100 and Value a range 0-100.

For filtering a certain colour in a image we define the ranges of the colour that has to be filtered. Every pixel is checked whether it is within this range, if so the pixel in the result image is set to 1 otherwise to 0. This result image is a binary image, where the colours in range of the colour are set to white. Colour filtering reduces the amount of noise caused by other colours in the image.

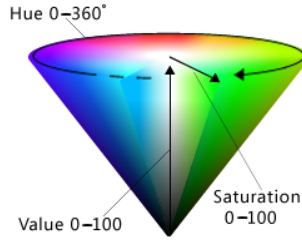


Figure 3: The HSV model, a cone having three parameters: Hue, Saturation and Value.

2.1.2 Canny Edge Detector

The Canny Edge Detector [Canny, 1986] is an edge detection operator that uses a multi-stage algorithm to detect edges. The aim of Canny was to develop a edge detector algorithm that is optimal for the following aspects:

Good detection by marking the most real edges in the image.

Good localization by marking the edges as close to the real edge.

Minimal response by only marking edges once.

Calculus of variations, a mathematical technique that finds the optimal function, was applied to fulfil these requirements. The algorithm consists of the following four stages in order to reach edge detection: Noise reduction, finding the intensity gradient, non-maximum suppression and hysteresis threshold. These stages will be explained in the next sections.

Noise reduction

Noise reduction is applied to raw image data as the edge detector is sensitive to noise. Noise reduction can be realized by using convolution with a suitable kernel. The Canny edge detector uses a Gaussian kernel as this is a suitable kernel. This phenomenon is called Gaussian Smoothing (see appendix B) and filters out the small distortions so these are not detected by the edge detector. Gaussian Smoothing results into a smoothed image.

Finding the intensity gradient

After the noise reduction the directional change in intensity, the gradient, is calculated for every pixel in the image. The gradient of every pixel in the image may point in a variety of directions. Therefore, the Canny Edge Detector uses four filters to detect horizontal, vertical and diagonal edges in the smoothed image. In order to find the gradient in the image the algorithm uses a edge detection operator, which takes the first derivative of the image that results in the gradient in horizontal direction G_x and vertical direction G_y . There are a variety of edge detection operators and the one applied in this thesis is the Sobel operator. The Sobel operator convolves (see appendix B) two 3×3 kernels with the image A to find the horizontal G_x and vertical G_y derivative, which is described in equation 1.

$$G_x = \begin{bmatrix} -1 & 0 & 1 \\ -2 & 0 & 2 \\ -1 & 0 & 1 \end{bmatrix} * A \quad G_y = \begin{bmatrix} -1 & -2 & -1 \\ 0 & 0 & 0 \\ 1 & 2 & 1 \end{bmatrix} * A \quad (1)$$

From the derivatives the gradient G and direction Θ can be determined, this is illustrated in equation 2.

$$G = \sqrt{G_x^2 + G_y^2} \quad \Theta = \arctan\left(\frac{G_x}{G_y}\right) \quad (2)$$

The directional angle is rounded to one of the four angles representing vertical, horizontal or the two diagonals in order to reduce computational costs of the algorithm.

Non-maximum suppression

Non-maximum suppression is the process of scanning a image along the image gradient direction. The pixels that are not part of the local maxima are set to zero. This suppresses all image information that is not part of the local maxima. Given the image gradient and direction estimates the algorithm seeks for the local maxima in the gradient direction by looping over the pixels of the image. For example, if the rounded gradient angle of the pixel is zero degrees, the pixel pointing downwards, the gradient magnitude is compared to the gradient magnitude of its left and right neighbour. If the gradient magnitude of the pixel is greater than its neighbours it will be considered a possible edge. Non-maximum suppression removes pixels that are not considered to be part of an edge. Therefore, only thin lines, candidate edges, will remain. This stage results in a binary image containing a set of possible edge points.

Hysteresis thresholding

The large intensity gradients are more probable to correlate to edges than small intensity gradients. For this reason, it is impossible to specify a threshold to determine whether a certain gradient is a edge or not. Therefore, the Canny Edge Detector applies another technique, namely, thresholding with hysteresis. In thresholding with hysteresis a upper and lower threshold is defined. The algorithm makes the assumption that important edges should be along continuous curves in the image, which allows the algorithm to follow a faint section of a given line and to ignore a few noisy pixels that have large gradients. Thresholding with hysteresis selects edges on the following basis:

- All candidates above the upper threshold will be selected as edges
- All candidates below the lower will be refused as edges
- All candidates between the upper and lower threshold will only be selected if it is connected to a pixel that is above the upper threshold.

This is the final step of the Canny Edge Detector and results into a boolean image representing the edges in the image.



Figure 4: Left: Original image. Middle: Smoothed image. Right: Canny Edge Detector

2.2 Motion Detection Algorithm

Motion detection is a tool in Computer Vision that is applied to detect whether an object has changed its position relative to its surroundings or the surroundings have changed relative to an object. Motion can be detected by mechanical and electronic methods. This is done by various sensors such as: sound, ultrasonic and opacity. Motion can be detected electrically via optical or acoustical detection. This thesis focuses on optical motion detection from the front camera as the platform has only a limited sensor suite (see chapter 4). This paper will focus on a algorithm that has been investigated for obstacle avoidance for the AR-Drone [Jurriaans, 2011]. In this approach optical flow is calculated to determine the disparity map with monocular stereo vision. This is done by using the resulting vectors of optical flow to calculate the fundamental matrix using RANSAC. The fundamental matrix serves as the input for the Hartley algorithm that generates a disparity map. This approach is explained in the following sections.

2.2.1 Shi-Thomasi

To find the optical flow in a set of images features have to be extracted from the current frame and be found in the next frame. A possibility that can provide decent features is the Shi-Tomasi algorithm. It tracks corners and defines a good feature in a similar approach as Harris, which depends on second-derivatives of image intensities. Calculating the autocorrelation of the second derivative over small windows around each point give a description of the window. According to Shi and Tomasi a good corner could be described by their eigenvalues as a good corner has eigenvalues that are greater than a minimum threshold.

As the images have a low resolution (see chapter 4), the sub-pixel corner locations are calculated as the intensity peak is almost never centred on a pixel. By fitting a parabola on the intensity of the window and find the maximum of this parabola to determining the sub-pixel location.

2.2.2 Optical Flow

Optical flow is the apparent motion between an observer and the environment. A example of calculated optical flow can be seen in figure 5. The algorithm tries to find the location of each pixel from one frame in the second. However, it is a challenging task to find corresponding pixels as many have the same colour and similar surrounding pixels. In order to calculate the optical flow mostly the assumption is made there is only a small movement between frames. In sparse optical flow, the most identical features are tracked across the images. Lucas-Kanade is an algorithm that makes this assumption, nonetheless it is able to track features over any distance due its pyramidal implementation.

Lucas-Kanade Pyramidal approach

The Lucas-Kanade algorithms makes the assumption that there is only small movement in frames in order to hold equation 3 when small windows are taken.

$$\begin{aligned} I_x(q_1)V_x + I_y(q_1)V - y &= -I_t(q_1) \\ I_x(q_2)V_x + I_y(q_2)V - y &= -I_t(q_2) \\ &\vdots \\ I_x(q_n)V_x + I_y(q_n)V - y &= -I_t(q_n) \end{aligned} \tag{3}$$

In this equation q_i stands for the pixels, $I_x(q_i)$, $I_y(q_i)$ and $I_t(q_i)$ are the partial derivatives of the image I for positions x , y and time t for q_i . These equations can be put in matrix form as

is shown in equation 4.

$$\begin{aligned}
 & Av = b \\
 A &= \begin{bmatrix} I_x(q_1) & I_y(q_1) \\ I_x(q_2) & I_y(q_2) \\ \vdots & \vdots \\ I_x(q_n) & I_y(q_n) \end{bmatrix} \\
 v &= \begin{bmatrix} V_x \\ V_y \end{bmatrix} \\
 b &= \begin{bmatrix} -I_t(q_1) \\ -I_t(q_2) \\ \vdots \\ -I_t(q_n) \end{bmatrix}
 \end{aligned} \tag{4}$$

This system is usually over-determined because it has more equations than unknowns. Lucas-Kanade algorithm obtains a compromise solution given by the least-square fit (see equation 5).

$$v = (A^T A)^{-1} A^T b \tag{5}$$

The least square fit gives the same importance to each pixel in the window. However, practice has shown that generally it is more efficient to increase the weight of the centre pixels in the window. This is done by adding a weight matrix W , which is a matrix containing all the weights for each pixel. This results in equation 6.

$$v = (A^T W A)^{-1} A^T W b \tag{6}$$

By gradually increasing the size of the window the optical flow over larger distances can be calculated as a least squares fit is found. A example of optical flow can be seen in figure 5.

Figure 5: Left: Frame one. Middle: Frame two. Right: Optical flow.

2.2.3 Fundamental Matrix with RANSAC

The fundamental matrix relates to the correspondence of each pixel location in two frames. This means that it can give the location of each pixel in one frame to the location of that pixel in the other. Together with the physical relation between two frames, the fundamental matrix can be used to calculate the essential matrix that provides information about the physical coordinates.

In order to determine the fundamental matrix RANdom SAmple Consensus (RANSAC) is used to discriminate outliers. RANSAC takes a subset of the points and fits a model on this subset. The model is evaluated by calculating whether the remaining points are inliers or outliers. When a sufficient amount of inliers is found the model is re-determined based on all the inliers of the model. This model is then evaluated by comparing it to other models of different iterations. The model with the smallest error is kept and will be used as model. The advantage of RANSAC is that it performs well with outliers in the data.

2.2.4 Hartley's algorithm

After determining the fundamental matrix the images can be rectified without calibrations by using Hartley's algorithm. Hartley's approach attempts to find homographies that map epipoles to infinity while minimizing the computed disparities. This is achieved by matching points between the two frames, which implicitly contain the camera intrinsics. The problem of Hartley's approach is that it does not calculate scale. This causes 3-Dimensional reconstructions to be determined by a projective transformation. This means that different projections of an object can appear the same to the human eye, when looking at the configuration of feature points.

Hartley first calculates the epipoles using the relations $Fe_1 = 0$ for the left epipole and $(e_r)^T F = 0$ for the right epipole. Homography H_r will map the right epipole to the 2-Dimensional homogeneous point at infinity. The homography has seven constraints since scale cannot be computed. The four degrees of freedom require only three constraints to map to infinity. The four degrees have to be selected cautiously because most choices result in distorted images. To calculate translate T that will take a selected point of interest to the origin of the right image and the rotation R that will take the epipole to $(e_r)^T = (f, 0, 1)$ can be calculated as shown in equation 7.

$$H_r = \begin{bmatrix} 1 & 0 & 0 \\ 0 & 1 & 0 \\ -1/k & 01 \end{bmatrix} RT \quad (7)$$

The homography of the left epipole can be determined by aligning the rows. Aligning by minimizing the total distance between all matching points in the frames.

2.2.5 Stereo Matching

After calculating the fundamental matrix the disparity map can be computed between the two frames. In order to compute the disparity map, a stereo matching algorithm has to be performed. This paper uses a fast one-pass stereo matching algorithm [??]. The algorithm uses sliding sums of absolute differences between pixels in the left image, while the pixels in the right image are shifted by some varying amount of pixels.

2.3 Probabilistic Hough Transform

The Probabilistic Hough Transform (PHT) [Kiriyati et al., 1991] is a feature extraction technique, which is similar to the Standard Hough Transform (SHT). This method is applied after the pre-processing stage, which in this case is done by a edge detector or a motion detector. Due to noise caused by the image data or pre-processing stage there may be missing points on the desired curve in the image. The goal of PHT is to address this problem by grouping edges into object candidates by performing a voting procedure over a set of parametrized image objects. In PHT lines are described in polar coordinates, distance r and angle θ . In the polar coordinate system r is the length of the vector and θ is the angle between the origin and the vector pointing to the closest point on the line. The representation of the line in the polar coordinate system is as follows:

$$y = -\frac{\cos \theta}{\sin \theta}x + \frac{r}{\sin \theta} \quad (8)$$

Every line is associated with a pair (r, θ) , which is unique when $\theta \in [0, 2\pi]$ and $r \geq 0$. For every point (ie. (x_0, y_0)) in the image the lines that go through are the following pairs (r, θ) :

$$r(\theta) = x_0 \times \cos \theta + y_0 \times \sin \theta \quad (9)$$

This results in a unique sinusoidal curve for every point in the (r, θ) plane. The sinusoidal curves of points that lay on the same line will have a joint intersection at the parameters for that line. All line candidates have to pass a threshold of intersections to be selected. In contrary with the SHT, PHT takes only a subset of the points found at the pre-processing stage. For this reason, PHT is computationally faster.

2.4 Tracking

Tracking is the process of locating a object in multiple images. In line-following navigation it is important to receive feedback from the environment. If the visual system gives rapid feedback the system is able to react faster. For instance, when the line changes direction the platform has to adjust its angle. In order to obtain rapid visual feedback the detection method of the object should be agile.

In order to detect the line in a agile way a Region Of Interest (ROI) window is placed, once the line is found. A ROI is a selected subset of the image. The ROI is placed at the most probable place the line will appear in the next frame on the basis of the orientation of the line and motion of the platform. Since the platform is required to follow the line the ROI is frequently placed in the middle. A ROI decreases the computational costs of an algorithm as it minimizes the search window.

2.5 Navigation

After detecting a line in the image the platform is required to navigate towards the line and follow it. This process of monitoring and controlling the movement of the vehicle is called navigation. In order to navigate towards the line the trajectory has to be calculated. In order to not lose the line it is kept in the middle of the screen while navigating over it. This gives the system the following tasks:

1. Move towards the line in the correct orientation
2. Navigate over the line while making adjustments to keep it in the middle of the screen.

The line that is found gives coordinates (x_1, y_1) and (x_2, y_2) . The linear equation $y = mx + b$ can be determined from these coordinates. Given the formula of the line the adjustment can be calculated, which result in a angle θ and a translation x . However, flying towards the line can be done in several ways. In this paper the platform first flies on top of the line and then correct its orientation parallel to the line. When the platform is hovering in the correct orientation above the line it will move forward, while correcting its orientation accordingly to the line. If the platform moves to far from the line the platform will do the above step again. This is the control strategy for line-following navigation.

3 Related Work

This chapter gives an overview of the related research that has been done regarding autonomous navigation unmanned aerial vehicles. Small stable quadcopters have become affordable and research on this platform is moving towards more intelligent and autonomous applications. Various autonomous navigation methods have already been investigated in the field.

Corridor and Stair Following Corridor following is a task performed by robots for autonomous navigation in indoor environments (ie. the office). Recently, a new navigation method for the MAV [Bills et al., 2011] was introduced to navigate in the indoor environment based on single image perspective cues. This is in contrast with previous approaches where a 3D model is built before planning and control. This method first classifies the type of indoor environment and then the MAV navigates through the environment using vision algorithms based on perspective cues to estimate the desired direction. The environment is detected through a confidence classifier, where estimates of the stair and corridor algorithms are used to compute the confidence values. The highest confidence value, above a threshold, is deemed as the current environment. The corridor and stair algorithm both use the Canny edge detector and Probabilistic Hough Transform to acquire the line segments. The corridor algorithm then tries to determine the vanishing point in the image. The stair algorithm on the other hand tries to determine the middle of the stairs by looking at horizontal line segments of the stairs.

These vision-based methods allow MAVs to traverse corridors, stairs and corners on the basis of a small, light-weight camera, which makes them suitable for MAV with payload and power restrictions.

Power Line Inspection Power line inspection is an essential task for the maintenance of the electric grids, which is difficult due to the range of grid distributions. Over last years rapid development has been made owing to the need for fast, accurate, safe and low-cost power line inspection [Katrashnik et al., 2010]. One of the main requirements of power line inspection robot is to be able to maintain its position above the power line and to navigate over the power line. A vision-based power line following method has already been proposed [Golightly and Jones, 2005]. This algorithm makes use of the Hough Transform to detect the line segments in the image. On the basis of the vertical line segments the position of the system is adjusted. The main advantage of power line inspection is that the MAV is able to follow three lines, namely, the conductor. Therefore, it is easier to navigate over power lines as when one of the conductors is not detected, the MAV can adjust its position according to the other two.

Another recent approach [Li et al., 2008] in power line following is to apply a Pulse-Coupled Neural Network (PCNN) to remove the background in the image. Thereafter use the Hough Transform to detect the line segments and then k-means clustering is employed to discriminate power lines from other straight lines. The PCCN filter is a biological inspired approach based on the understanding of visual cortical models of small mammals. The PCCN filter is a great potential due to the low computational costs.

Road-Following Road-Following is a task performed by robots for autonomous navigation in outdoor environments. Small autonomous aircraft [Frew et al., 2004] have already been able to follow a road based on real-time road detection and localization. The algorithm uses multiple vision-based method to detect the road and the lane markings. First the Bayesian Pixel Classifier is applied on every pixel to see whether it belongs to the road.

The classifier makes use of a database of RGB values of over 20000 pixels. Then connected-component analysis is used by labelling pixels in order to remove noise in the image and detect connected regions. After detecting the road in the image the lane markings are detected by the Bayesian pixel classification algorithm. Then a Hough Transformation is applied to test multiple candidate lanes. This result in a rough discretization of the lan. Lastly, robust line fitting, least-trimmed square, is applied to finalize the position and orientation of the center lane markings. This resulted into encouraging results, however, improvements of the algorithm can still be made.

Obstacle avoidance Obstacle avoidance is a task of satisfying some control objective subject to non-collision position constraints. In obstacle avoidance the UAV requires to navigate around the obstacle to its objective. A recent approach was to achieve obstacle avoidance by a visual Fuzzy Logic serving system [Olivares-Mendez et al., 2012]. The vehicle obtains images from the front camera and processes them with the Camshift algorithm, a algorithm that is used to track a defined colour. Depending on the output of the vision system the Fuzzy Logic controller gives controls to the UAV.

Non-knowledge based methods have also been investigated for obstacle avoidance [Jurriaans, 2011]. The proposed method, discussed in section 2.2.2, is able to navigate through corridors and to avoid obstacles.

Elementary Motion Detectors A approach last year during the IMAV competition by the BioMAV team [Gerke et al., 2011] was to combine motion information provided by Elementary Movement Detectors (EMDs) with edge detection. EMDs are useful for UAVs due to the detection of temporal and motion effects caused by the flight. In combination with edge detection this method filters out noise caused by contrast differences in the image. From this cleaned image objects were detected by using a hough transform.

4 Platform: Parrot AR.Drone

One of the basic steps for the development and testing of intelligent applications in robotics is to find an applicable robot platform for the defined problem. A common choice is to use a quadcopter, which is mainly designed to be a Unmanned Aerial Vehicle (UAV). The small size and manoeuvrability allows both indoor and outdoor flights. Moreover, quadcopters have a simple design due to the fact that they do not require mechanical connections to vary the pitch angle of rotor blade. As a result of technological developments in aerospace engineering of UAV's, a small quadcopter with on-board stabilization can be purchased conveniently. Because of this, research regarding this platform is moving towards more intelligent applications, which demand information of the surrounding environment. The specific platform selected for the experiments in this research is the Parrot AR.Drone quadcopter. The advantages of this platform are its on-board stabilization, lightweight and the affordable price of the platform. The AR.Drone is carrying a front and bottom camera that provide live video streaming through the data link. Additionally, it has an ultrasound sensor and an inertial measurement unit that measures the pitch, roll, yaw and accelerations of the platform. The platform is controlled via WiFi, which allows the user to send commands and receive data of the platform. In this chapter, the AR.Drone platform is described. The operational part of the platform is discussed, the hardware the platform contains is described and the software development kit is briefly described.

4.1 Quadcopter

A quadcopter consists of four rotors that are attached to a main frame, which commonly has a cross-shaped form (see figure 6). Every rotor produces thrust T and torque τ over the center of rotation, whereas it also produces drag force D_b in the opposite direction of flight. Thrust T is the force that is generated by increasing and decreasing acceleration the mass in one direction. The acceleration of the mass will result in a force of equal magnitude but in the opposite direction of the platform. Torque τ is the force that rotates an object around its axis. Drag D_b is the force that is in opposite direction to the motion of the aircraft through air. This force is inclined on the velocity of the quadcopter and de-acceleration will take place if insufficient thrust is generated. The rotors together should generate sufficient thrust to stay airborne during flights.

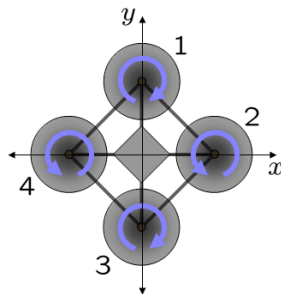


Figure 6: Diagram of the reaction torques on each motor of the quadcopter, due to the rotors. Rotors one and three are spinning clockwise, whereas rotor two and four spin counter-clockwise, causing opposing force for control

In order to fly the quadcopter relies on differences in thrust and torque. Pitch, roll and yaw (see figure 7) is the naming of flight dynamics to indicate the rotation angles in three dimension of the center mass of the quadcopter. The opposing rotor pairs (pair 1, 3 and pair 2, 4) turn

in the same direction. One of the pairs is turning clockwise, while the other pair turns counter-clockwise. This causes the platform to have no angular acceleration, when all rotor pairs have the same angular acceleration. Alternating the angular speed of the rotor pairs will cause angular acceleration about the yaw.

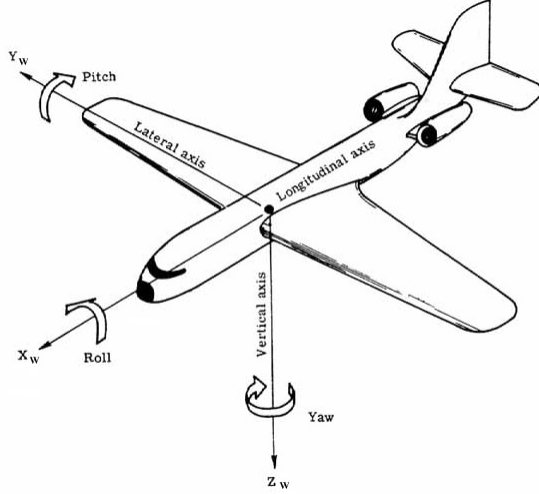


Figure 7: Diagram of pitch, roll and yaw rotations on an aerial vehicle

Vertical movements are accomplished by changing the thrust from each rotor alike, which is causing the resulting thrust to change and the differential torque to remain zero. Moreover, when the thrust is kept constant the vertical velocity remains the same. Horizontal movements are caused by changing the pitch and roll angle. Angular accelerations over the pitch and roll angles can be generated independently. Each pair of opposing rotors controls either pitch or roll rotation of the platform. A torque balance is kept for yaw stability during differential torque over the roll and pitch by increasing the speed of one rotor, while decreasing the speed of the opposing rotor.

4.2 Hardware

The AR.Drone is a remote-controlled quadcopter developed by the french company Parrot SA for consumer use. The main frame is made of carbon fibre and high resistance plastic. The AR.Drone has an indoor and outdoor hull, which is used for protection of the system. The rotors are powered by motors, whom are connected to a lithium battery allowing the system to fly ten minutes.

4.2.1 AR.Drone 1.0

The AR.Drone has an on-board computer running a custom Linux operating system. A mini-USB connector is included on the system for software maintenance and additional external sensors (e.g. GPS sensor). The integrated wireless card provides network access for external devices that control the vehicle. The software of the AR.Drone is available for all platforms, however, the most supported software is written for iOS devices (ie. Apple iPhone). Nevertheless, it is possible to create controlling applications for the Windows and Linux platforms. Furthermore,

the AR.Drone has a sensor suite containing an six degrees of freedom Inertial Measurement Unit (IMU), a bottom camera and a ultrasound altimeter used for automatic stabilization. The IMU consists of a three axis accelerometer, a two axis roll and pitch gyrometer and a single axis yaw gyrometer. The IMU reports on the system its velocity, orientation and gravitational forces. The ultrasound altimeter measure the altitude of the system and in combination with the bottom camera it calculates the optical flow of the system. All the above sensors contribute to the on-board stabilization module of the quadcopter, which allows the quadcopter to hover in one place. Additionally, the system carries a frontal camera to provide the operator with visual feedback.

The horizontal camera has approximately $75^\circ \times 60^\circ$ field of view and provides 640×480 pixel color images. The bottom camera provides color images with 176×144 pixels and its field of view is approximately $45^\circ \times 35^\circ$ [Krajník et al., 2011].

4.2.2 AR.Drone 2.0

Recently, Parrot brought a new platform on the market, the AR.Drone 2.0. This new platform has a similar configuration as its predecessor, however, most of the components have been improved. The new on-board technology gives better stabilization and more precise sensor measurement comparing to their previous platform. The AR.Drone two carries a horizontal camera with a resolution of 1280×720 pixels and the vertical camera a resolution of 320×240 pixels. These improvements aid intelligent vision-based applications as more detailed images give more information about the environment.

4.3 Software Development Kit

Parrot created a open source Software Development Kit (SDK) providing developers the opportunity to create intelligent applications for their platform. The SDK comes with source code, multiplatform examples and documentation. The SDK does not provide software that is embedded on the AR.Drone itself. The SDK implements the following three channels of communications with the platform:

1. Configuration and control of the platform.
2. Status of the platform (ie. altitude, attitude and speed).
3. Video stream.

These four channels of communication can be used for designing intelligent applications for the AR.Drone.

5 Framework: AR.Drone SLAM

In this chapter, the functionality and architecture of the development framework AR.Drone SLAM [Dijkshoorn, 2012] will be briefly described. The framework allows the performance of advanced tasks (ie. automated drone control) in real-time. The framework consists of an abstraction layer that allows the user to test methods in simulation and in real. The framework is built modular so new methods can be easily integrated into the framework.

5.1 Functionalities

The framework has the following main functionalities:

- Object-oriented: the robot and the various methods are represented by objects.
- Abstraction: the framework can be used in a real and simulated environment.
- Replay: the framework is able to record and replay datasets.
- Independent sensor and data processing.
- Various controllers: keyboard and 3D mouse.
- Autonomous way-point navigation.
- Real-time 3D map visualization of the environment.
- Simple communication with AR.Drone
- Access to Computer Vision library OpenCV.

The simulated environment the framework has access to is USARSim³. USARSim is a high-fidelity simulation of robots and environments based on the Unreal Tournament game engine. In USARSim a model of the AR.Drone is available and new environments can be created easily. Therefore, it allows methods to be evaluated in various environments. Furthermore, the framework has access to the AR.Drone via the provided SDK. This gives full control over the drone.

Due to the functionalities of the framework it is suitable for developing and testing vision-based methods. This is for the reason that a new module can simply be integrated into the framework. After the integration the method can then first be evaluated in simulation before testing it in real. This provides more certainty whether the developed method will work in real. Furthermore, the resources (ie. localization) the framework provides can aid the methods of navigation.

5.2 Architecture

The framework consists of several components, which are illustrated in figure 8. Here the various components will be described:

Main application this is the place, where the configurations (ie. controller and environment) are set of the programme.

Bot the main representation of a robot in the framework. The bot has access to all functionalities

³<http://usarsim.sourceforge.net>

Controllers the behaviour, 3D mouse and keyboard controller are implemented here and control the drone.

Interfaces the USARSim and ARDroneLib are the interfaces for the communication between the framework and the simulated or real AR.Drone.

Modules the modules sensor, frame, modules and UI implement the various implemented functionalities of the framework.

Record/Playback allows datasets to be recorded and replayed.

Integrating a new module in the framework is simple as this basically expands the functionality of the robot.

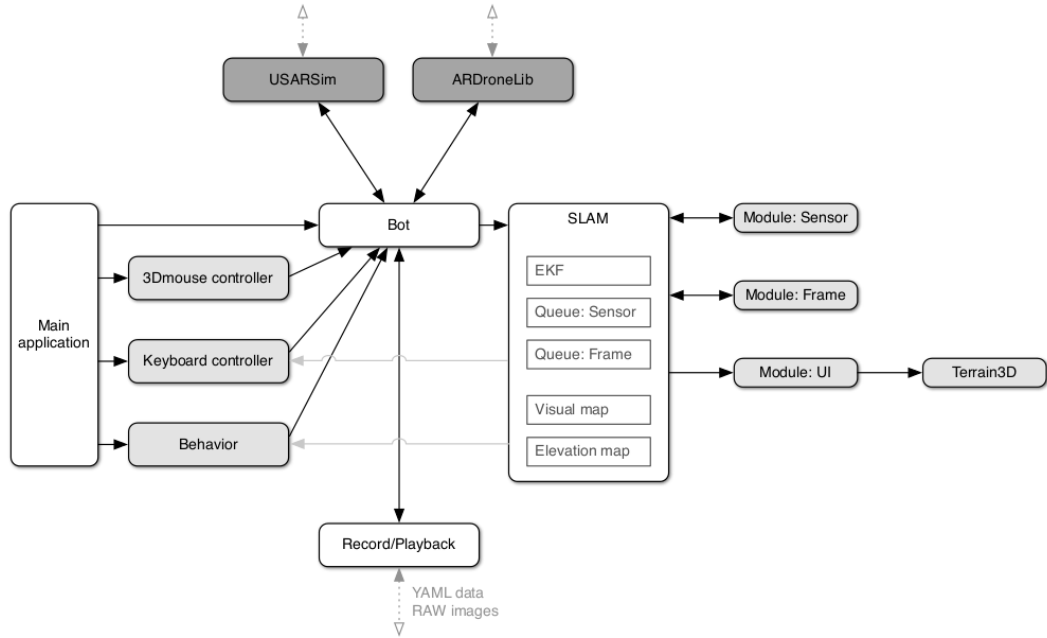


Figure 8: Schematic overview [Dijkshoorn, 2012] of the development framework AR.Drone SLAM

6 Methods and Experiments

This chapter describes the methods and experiments that lead to autonomous line-following. The proposed methods and experiments aid to answer the previously determined research questions (see chapter 1.3). The various designer choices, configurations, datasets and evaluation criteria will be discussed in this chapter.

6.1 Platform

For this paper, the Ascending Technologies Pelican (see appendix C) and Parrot AR.Drone (see chapter 4) were both considered for the evaluation of the vision-based algorithms. To evaluate the algorithms a stable platform with on-board stabilization was required. The Pelican has several advantages such as: on-board processing, modular design and high payload. However, the system has no indoor on-board stabilization and had technological difficulties with the wireless connection. Therefore, the Parrot AR.Drone was chosen to perform during the experiments.

6.2 Optimal Camera Configuration

In order to perform vision-based line-following navigation the optimal camera configuration has to be determined. In the current configuration of the AR.Drone it has a bottom and front camera. For optimal line-following navigation the camera has to point obliquely to the ground in front of the MAV. This for the reason that the platform should look ahead of itself so it can adjust itself on time. Neither the bottom or front camera provide this view as the bottom camera has a small field of view and the front camera looks too far ahead. This makes it impossible for the drone to navigate over a line as the platform cannot adjust itself in time to changes or not even able to detect the line. Therefore, the current configuration of the cameras is not suitable for navigation.

The optimal solution for the camera configuration would be the pan-tilt camera of the Pelican. The pan-tilt camera can change the angle of the camera and therefore suitable for flying at various altitudes. Since the experiments are only indoors the platform only flies at altitudes between 1-2 metres. Therefore, a angle of approximately 45° is considered and tested in this paper. In order to change the angle this thesis constructed and tested the following two solutions to change the angle:

Mirror construction A mirror construction that changes the view of the front camera. This construction can be placed on top of the front camera. The mirror has an angle towards the ground, which gives the camera the mirrored ahead view.

Modification of AR.Drone Modify the position of the front camera. Due to the fact that the AR.Drone is made from styrofoam its simple to modify the angle of the front camera. By cutting away styrofoam its possible to set the camera under a different angle.

6.3 Determining line to follow

6.4 Experiments

To compare the two vision-based algorithms two types of experiments have been designed. The experiments (see figure 9) challenge both the algorithms. In experiment one the weakness of the motion detection algorithm is challenged by putting a orange line on the ground, while in experiment two the edge detection algorithm is challenged by hanging a blue coloured line in the air with a blue background.



Figure 9: Left: Setup of experiment one. Right: Setup of experiment two

6.5 Evaluation Criteria

6.6 Hypothesis

- Ontwerpbeslissing voor lijn vindenn
- Optimale configuratie camera
- Opstellingen
- Evaluatie criteria
 - Frames met lijn
 - Nauwkeurigheid directie van de lijn
- Vaste datasets om goed te kunnen evalueren zodat ik niet onnauwkeurigheid navigatie meeneem.

7 Results and Discussion

- Tabellen met resultaten
- Gemiddelde afwijking
- Standaard derivatie
- camera kijkt vooruit
- waarom resultaten zo zijn

8 Conclusion

- Optimaal algoritme bestaat niet
- Frame als indicatie gebruiken

8.1 Future works

- Combinatie algoritme
- Testen in meer environments
- Meer algoritmes testen
- Meer Criteria
- Navigatie oplossen
- Tracking
- Evaluatie criterium navigatie

Appendices

A Source code

All the source code is available at the GitHub repository:

<https://github.com/camielv/ThesisVerschoor>.

The recorded datasets are available here:

<https://github.com/camielv/ThesisVerschoor/Datasets>

A research log can be found here:

<http://camielv.nl/thesis>

B Gaussian Smoothing

This chapter provides a explanation for Gaussian Smoothing. The convolution technique is discussed first and then the Gaussian kernel of convolution is explained.

Convolution

Convolution is a mathematical way to combine two functions. The mathematical definition of convolution for the two scalar functions $f(x)$ and $g(x)$ is:

$$h(x) = \int_{-\infty}^{\infty} f(u)g(x-u)du$$

The integral expresses the amount of overlap of function $g(x)$ due the shift over the other function $f(x)$. This causes one function to blend with the other. The convolution operator contains the following algebraic properties: commutativity, associativity and distributivity. Convolution is commonly applied in computer vision in order to detect edges in a image. In figure 10 a example of a convolution with the Gaussian Kernel is illustrated.



Figure 10: Left: original. Middle and right: Gaussian Blur of 11 and 22 pixels.

Gaussian Kernel

The most suitable kernel for an optimal convolution is the Gaussian function due to the smoothing, derivatives and separability. The Gaussian function has the best smoothing properties as it has existing derivatives to any order at every point. Due to this every function can be smoothed as the derivative is always non-zero. In image processing the intensity is smooth smoothed intensity of a image this can be done by convolving the original image with the derivative of the Gaussian function. Gaussian Smoothing is the result of blurring an image by a Gaussian Function. Smoothing is applied to reduce noise and detail in the image. Gaussian smoothing is a well know technique mostly used in computer vision algorithms as a pre-processing technique in order to enhance image structures at different scales. Gaussian Smoothing is the same as convolving the image with a Gaussian function. The 2D Gaussian smoothing function is represented by the following equation:

$$G(x, y) = \frac{1}{2\pi\sigma^2} e^{-\frac{x^2+y^2}{2\sigma^2}}$$

C Ascending Technologies Pelican

To be written.

9 Bibliography

- [Bajaj et al., 2002] Bajaj, R., Ranaweera, S., and Agrawal, D. (2002). Gps: location-tracking technology. *Computer*, 35(4):92–94.
- [Bills et al., 2011] Bills, C., Chen, J., and Saxena, A. (2011). Autonomous mav flight in indoor environments using single image perspective cues. In *Robotics and Automation (ICRA), 2011 IEEE International Conference on*, pages 5776–5783.
- [Bradski and Kaehler, 2008] Bradski, G. and Kaehler, A. (2008). *Learning OpenCV*. O'Reilly Media Inc.
- [Canny, 1986] Canny, J. (1986). A computational approach to edge detection. *Pattern Analysis and Machine Intelligence, IEEE Transactions on*, PAMI-8(6):679–698.
- [Dijkshoorn, 2012] Dijkshoorn, N. (2012). Simultaneous localization and mapping with the ar.drone. Master's thesis, Universiteit van Amsterdam.
- [Dupuis and Parizeau, 2006] Dupuis, J. and Parizeau, M. (2006). Evolving a vision-based line-following robot controller. In *Computer and Robot Vision, 2006. The 3rd Canadian Conference on*, page 75.
- [Frew et al., 2004] Frew, E., McGee, T., Kim, Z., Xiao, X., Jackson, S., Morimoto, M., Rathinam, S., Padial, J., and Sengupta, R. (2004). Vision-based road-following using a small autonomous aircraft. (3).
- [Gerke et al., 2011] Gerke, P., Langevoort, J., Lagarde, S., Bax, L., Grootswagers, T., Drenth, R.-J., Slieker, V., Vuurpijl, L., Haselager, P., Sprinkhuizen-Kuyper, I., Otterlo, M., and de Croon, G. (2011). Biomav: bio-inspired intelligence for autonomous flight. In *Proceedings of the International Micro Air Vehicle conference and competitions, 12-15 September (IMAV 2011)*.
- [Golightly and Jones, 2005] Golightly, I. and Jones, D. (2005). Visual control of an unmanned aerial vehicle for power line inspection. In *Advanced Robotics, 2005. ICAR '05. Proceedings, 12th International Conference on*, pages 288–295.
- [Grasmeyer et al., 2001] Grasmeyer, J. M., Keenon, M. T., and Inc, A. (2001). Development of the black widow micro air vehicle. In *39th AIAA Aerospace Sciences Meeting and Exhibit*.
- [Jurriaans, 2011] Jurriaans, R. (2011). Flow based obstacle avoidance for real world autonomous aerial navigation tasks. Bachelor's thesis, Universiteit van Amsterdam.
- [Katrásník et al., 2010] Katrásník, J., Pernus, F., and Likar, B. (2010). A survey of mobile robots for distribution power line inspection. *Power Delivery, IEEE Transactions on*, 25(1):485–493.
- [Kiryat et al., 1991] Kiryat, N., Eldar, Y., and Bruckstein, A. (1991). A probabilistic hough transform. *Pattern Recognition*, 24(4):303–316.
- [Krajník et al., 2011] Krajník, T., Vonásek, V., Fišer, D., and Faigl, J. (2011). AR-Drone as a Robotic Platform for Research and Education. In *International Conference on Research and Education in Robotics*, Heidelberg. Springer.
- [Li et al., 2008] Li, Z., Liu, Y., Hayward, R., Zhang, J., and Cai, J. (2008). Knowledge-based power line detection for uav surveillance and inspection systems. In *Image and Vision Computing New Zealand, 2008. IVCNZ 2008. 23rd International Conference*, pages 1–6.

- [Olivares-Mendez et al., 2012] Olivares-Mendez, M. A., Mejias, L., Campoy, P., and Mellado-Bataller, I. (2012). Quadcopter see and avoid using a fuzzy controller. In *The 10th International FLINS Conference on Uncertainty Modeling in Knowledge Engineering and Decision Making (FLINS 2012)*, Istanbul, Turkey. World Scientific.
- [Sampei et al., 1995] Sampei, M., Tamura, T., Kobayashi, T., and Shibui, N. (1995). Arbitrary path tracking control of articulated vehicles using nonlinear control theory. *Control Systems Technology, IEEE Transactions on*, 3(1):125 –131.
- [Ziou and Tabbone, 1998] Ziou, D. and Tabbone, S. (1998). Edge detection techniques - an overview. *International Journal of Pattern Recognition and Image Analysis*, 8:537–559.